A Branch-independence-based Reliability Assessment Approach for Transmission Systems

Shuonan Hou, Pei Zhang, Wei Zhang, Qian Xiao, and Xiaonan Liu

***Abstract*—This paper proposes a branch-independence-based reliability assessment approach for transmission systems. The approach consists of branch decoupling and state-space partition techniques. By integrating an impact-increment-based reliability index calculation model and the proposed branch decoupling technique, a proportion of sampled contingency states no longer need to be analyzed using the time-consuming optimal power flow (OPF) algorithm. In this way, the technique speeds up the calculation of reliability indices. Since first-order contingency states have a high probability of being sampled, we propose a state-space partition technique to replace first-order contingency state simulation with first-order contingency state enumeration. Consequently, the calculation of reliability indices is further accelerated by avoiding a large amount of repetitive OPF analyses during simulation process without affecting reliability index accuracy. The validity and applicability of our approach are verified using the IEEE 118-bus and IEEE 145-bus systems. Numerical results indicate that the proposed approach can improve computational efficiency without decreasing accuracy.**

***Index Terms*—Branch decoupling, impact increment, optimal power flow (OPF), reliability assessment, state-space partition, transmission system.**

I. Introduction

RELIABILITY assessment is essential for transmission system planning. The reliability indices can be accurately calculated with consideration of the probabilities and impacts, i.e., severities, of all states. However, the impact of a contingency state needs to be calculated using the optimal power flow (OPF) algorithm, which is a time-consuming process. In addition, the number of contingency states can be enormous, as it increases exponentially with the system scale. Therefore, the OPF analysis can only be performed for a portion of contingency states, which may introduce remarkable reliability index errors. It is a long-term goal and a great challenge for researchers to obtain accurate reliability indices with high computational efficiency.

Many reliability assessment methods have been developed in recent decades. According to different state selection techniques and reliability index formulations, the reliability assessment methods for transmission systems are generally categorized into state enumeration (SE) method and Monte Carlo simulation (MCS) method. The traditional SE method enumerates contingency states up to a given order (usually the second or third), computes the corresponding probability and impact for each enumerated state, and calculates the reliability indices by accumulating the product of the probability and impact [1], [2]. The SE method may not yield accurate reliability indices due to the omission of higher-order states, especially when evaluating large-scale or low-reliability power systems. Although some techniques such as fast sorting [3], [4], contingency screening [5] - [7], and contingency ranking [8] have been developed to address this problem, SE method is more suitable for small-scale or high-reliability systems.

MCS method can be divided into sequential MCS and non-sequential MCS depending on whether chronological characteristics are considered. Compared with sequential MCS, non-sequential MCS has a much smaller computational burden, making it be used more widely. This paper only focuses on non-sequential MCS. The traditional non-sequential MCS extracts individual states from the state space based on component availability, calculates the impact of each sampled contingency state, and iteratively updates the average impact of all sampled states to obtain reliability indices until the given stopping criterion is satisfied [9]. The method converges if the stopping criterion is strict enough. In this case, the reliability indices obtained are accurate and credible. The statistical characteristic makes MCS method more suitable for evaluating large-scale systems. However, in the case of significant simulation variance, a considerable amount of OPF analyses must be performed to make the method converge, leading to the inefficient computation of reliability indices. To address this issue, some techniques such as state-space pruning [10], [11], importance sampling [12], subset simulation [13], and cross-entropy [14], [15] have been developed to improve sampling efficiency, i.e., to reduce the sample size required for convergence. Moreover, some state classification techniques [16]-[18] have been developed to classify a proportion of contingency states into failed states, i.e., loss of load states, and success states by a

Manuscript received: April 28, 2021; revised: August 2, 2021; accepted: November 8, 2021. Date of CrossCheck: November 8, 2021. Date of online publication: January 6, 2022.

This work was supported by the China Postdoctoral Science Foundation (No. 2020TQ0222).

S. Hou and Q. Xiao are with the Key Laboratory of Smart Grid of Ministry of Education, Tianjin University, Tianjin, China (e-mail: shuonan_hou@tju.edu.cn; xiaoqian@tju.edu.cn).

P. Zhang is with the School of Electrical Engineering, Beijing Jiaotong University, Beijing, China (e-mail: 2512692577@qq.com).

W. Zhang (corresponding author) is with the State Key Laboratory of Information Photonics and Optical Communications, Beijing University of Posts and Telecommunications, Beijing, China (e-mail: weizhang13@bupt.edu.cn).

X. Liu is with the State Grid Tianjin Electric Power Research Institute, Tianjin, China (e-mail: xiaonanliu@tju.edu.cn).

DOI: 10.35833/MPCE.2021.000242

small amount of computation. During the simulation, success states no longer require the OPF analysis, thus improving the computational efficiency.

The above techniques do not exploit the connection between state impacts to improve the accuracy and computational efficiency of reliability indices. In [19], an impact-increment-based reliability index calculation model has been proposed and combined with the SE method to perform the reliability assessment for integrated energy systems. This model can increase the contribution of lower-order states to the reliability indices by transferring partial impacts of higher-order states to those of the corresponding lower-order ones. In this way, the reliability indices obtained by state enumeration are more accurate. In [20], an incremental reliability assessment approach has been proposed to efficiently calculate the reliability enhancement, i.e., the incremental reliability indices, brought by the planned scheme to the existing system. The approach takes advantage of the impact correlation between the added components and existing components to separate the incremental reliability indices from the entire reliability indices and reduce the set of states that may have a contribution to the incremental reliability indices. In this way, the reliability enhancement brought by the planned scheme can be quickly quantified. However, for this approach, the planned scheme is limited to add branches to the existing system. Moreover, the load level of the planned system must be the same as that of the existing system. The two constraints narrow the applicability of this approach. In [21], a contingency set partition based impact transfer approach has been developed to improve the sampling efficiency. With this approach, lower-order states are separated from sample space, which prevents these high probability states from being repeatedly sampled. Based on this separation, the differences between non-zero impacts and zero impacts of higher-order states are reduced by impact transfer, which lowers the higher-order simulation variance and further improves the sampling efficiency.

For modern power system planning, the accuracy or efficiency improvement brought by existing techniques is not enough. As modern power systems become more and more complex, the computational burden of OPF increases. Besides, in optimal planning, the reliability assessment needs to be done repetitively. In extreme natural disasters, the system reliability information needs to be updated quickly. Therefore, a higher computational efficiency is required for reliability assessment while ensuring the accuracy of reliability indices.

Based on the impact-increment-based reliability index calculation model in [19], this paper proposes a branch-independence-based reliability assessment (BIRA) approach to further improve the computational efficiency of transmission reliability assessment. The BIRA approach consists of branch decoupling (BD) and state-space partition (SSP) techniques. The BD technique takes advantage of the weak power flow coupling between certain branches to reduce the number of OPF analyses. If the outage branches of a branch outage state can be decoupled into two independent branch sets, this state does not need to be analyzed with OPF. The branch outage state refers to a contingency state where no generation unit fails. Since the first-order states have a high probability of being sampled and cannot be handled by BD technique, these states are separated from sample space by SSP technique to further improve the computational efficiency. With the SSP technique, the simulation of the first-order states is replaced by the enumeration of the first-order states. This avoids repetitive OPF analyses of the first-order states. In addition, a new reliability index formulation is derived considering the adaptation to SSP technique.

The rest of this paper is organized as follows. Section II introduces the impact-increment-based reliability index calculation model. The BIRA approach is proposed in Section III. Case studies are presented in Section IV, and conclusions are drawn in Section V.

II. Impact-increment-based Reliability Index Calculation Model

Compared with the traditional reliability index calculation model, the impact-increment-based reliability index calculation model transforms state impact into modified impact increment. The transformation increases the contribution of lower-order states to the reliability index. Let R represent the reliability index. This model is expressed as:

$$R = E\left(I_s | s \in S\right) = E\left(\Delta I_s' | s \in S\right) = \sum_{s \in S} P_s \Delta I_s' \tag{1}$$

where S is the state space of the evaluated system; s is a state denoted by the set of corresponding outage components, when $s = \varnothing$, it is the normal state, otherwise, it is a contingency state; P_s is the state probability; I_s is the state impact, which is obtained by OPF analysis; and $\Delta I_s'$ is the modified impact increment, which can be expressed as:

$$\Delta I_s' = \frac{\Delta I_s}{\prod_{j \in C-s} a_j} \tag{2}$$

where a_j is the availability of component j; C is the set of all components in the system; $C-s$ is the set of components excluding the outage components corresponding to state s; and ΔI_s is the impact increment, which can be expressed as:

$$\Delta I_s = \sum_{k=1}^{n_s} (-1)^{n_s - k} \sum_{u \in \Omega_s^k} I_u \tag{3}$$

where n_s is the number of outage components corresponding to state s; u is a lower-order state corresponding to state s; and Ω_s^k is a set of k^{th}-order states corresponding to state s, which can be expressed as:

$$\Omega_s^k = \left\{ v | v \subset s, Card(v) = k \right\} \tag{4}$$

where v is a lower-order state corresponding to state s; $Card(v)$ is the cardinality of v.

It should be noted that this model must be combined with a state selection method such as SE or MCS to complete reliability assessment. The IISE method represents the combination of SE method and this model. Similarly, the IIMCS method represents the combination of MCS method and this model.

III. BIRA Approach

A. BD Technique

Based on the impact-increment-based reliability index cal-

culation model, the BD technique takes advantage of branch relations to reduce the number of OPF analyses required by the IIMCS method. The cooperation mechanism of the BD technique and IIMCS method is illustrated in Fig. 1. The IIMCS method consists of three basic steps, i.e., state selection, state analysis, and reliability index calculation. Before embedding BD technique, the IIMCS method must perform the OPF analysis for each sampled contingency state to obtain the state impact. After embedding the BD technique, a proportion of the sampled contingency states are screened out. The OPF analyses of these states can be avoided. The BD technique estimates the relations (including dependence or independence) between all branches and records the branch relations in a matrix. Thereafter, the relations between the outage branches of a sampled contingency state are obtained from the matrix. It is important to note that the BD technique can only handle the contingency state with the outage order higher than 1. Finally, the BD technique determines whether the outage branches of the state can be decoupled according to the branch relations. If the outage branches can be decoupled into two independent branch sets, the modified impact increment of this state can be obtained directly. Otherwise, the state should be analyzed with the OPF algorithm. The BD technique significantly reduces the computation effort of reliability assessment by reducing the number of OPF analyses. In the following, we first propose the definition of branch relations and two theorems as the theoretical foundation of the BD technique. After that, branch relation estimation and branch decoupling determination are introduced.

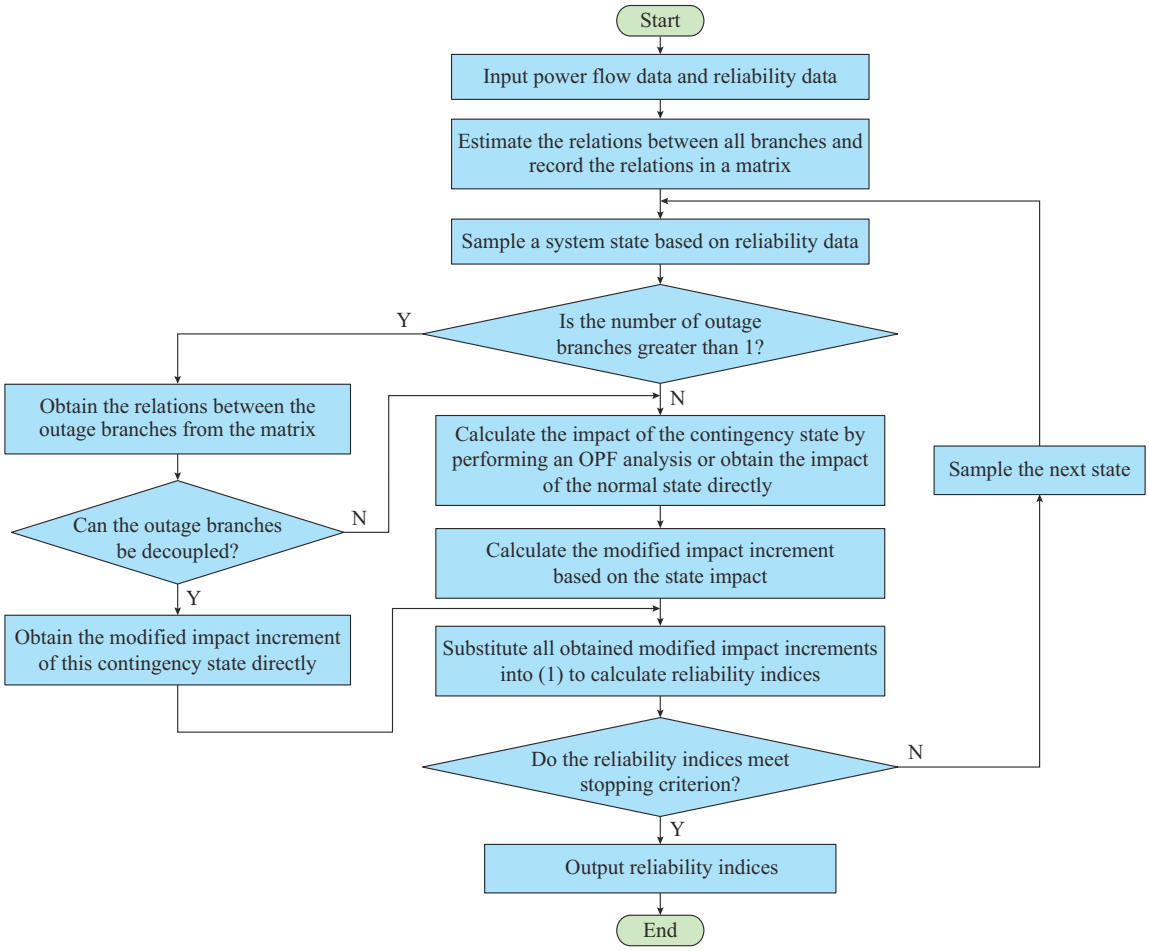

Fig. 1. Cooperation mechanism of BD technique and IIMCS method.

The definition of branch relations is proposed as follows. The outage of a branch (including line or transformer) set changes power flow distribution. If two branch sets have no common branch, and their outages cannot affect the power flow on the same branch, these branch sets are independent. Conversely, if their outages affect the power flow on the same branch, these two branch sets are dependent. In other words, branch independence is that there is no power flow coupling between two branch sets. In practical utilization, if the power flow coupling between two branch sets is weak enough, these branch sets are considered independent.

An example system in Fig. 2 is used to illustrate the definition of relations between branches. The generation unit is considered to be 100% available and have adequate power. The transmission lines are considered to have sufficient transmission capacity. According to the network structure, the outage of Line 1 affects only the power flow on Line 1 and accordingly causes a load curtailment of 5 MW on Bus 1. The outage of Line 2 affects the power flow on Line 2 and Line 3. The corresponding load curtailments on Bus 2

and Bus 3 are 6 MW and 8 MW, respectively. The outage of Line 3 affects the power flow on Line 2 and Line 3. The corresponding load curtailment on Bus 3 is 8 MW. Therefore, the outages of branch sets $\{1\}$ and $\{2,3\}$ cannot affect the power flow of the same branch. The outages of branch sets $\{2\}$ and $\{3\}$ can affect the power flow of the same branch. According to the definition of branch relations, branch sets $\{1\}$ and $\{2,3\}$ are independent; while branch sets $\{2\}$ and $\{3\}$ are dependent.

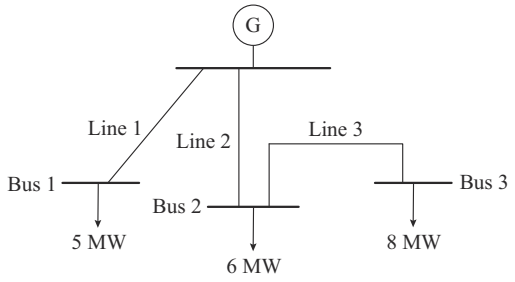

Fig. 2. Example system for illustrating definition of relations between branches.

According to Fig. 2, we can obtain:

$$I_{\{1\}}+I_{\{2,3\}}=5+14=19=I_{\{1,2,3\}} \tag{5}$$

$$I_{\{2\}}+I_{\{3\}}=14+8\neq 14=I_{\{2,3\}} \tag{6}$$

where $I_{\{\cdot\}}$ is the outage impact of branch set $\{\cdot\}$. In other words, if all branches in branch set $\{\cdot\}$ are out of service, the outage impact is $I_{\{\cdot\}}$. In the rest of this paper, the outage impact of a branch set is simply referred to as the impact of a branch set. Besides, since the outage of a branch set corresponds to the occurrence of a specific contingency state, this branch set can be used to represent the contingency state. Thus, the impact of this branch set is equivalent to the state impact.

According to (5) and (6), we can suppose that the impacts of two independent branch sets have superposition property. An impact superposition theorem is proposed as follows. Let A and B represent two branch sets. Let I_A and I_B represent the impacts of A and B, respectively. If A and B are independent, the sum of I_A and I_B can be expressed as:

$$I_A+I_B=I_{A\cup B} \tag{7}$$

where $I_{A\cup B}$ is the impact caused by the simultaneous failure of A and B.

The impact superposition theorem is confirmed by the explanation that outage branches no longer have power transmission capacity. If the load on outage branches cannot be transferred, or if some branches are overloaded due to load transfer, the system must reduce the load. The load curtailment is the branch outage impact. Suppose A is branch set $\{i,j\}$, and the outage of A changes the power flow on branches i, j, k, l. Let P_{mk} and P_{ml} represent the maximum transmission capacities of k and l, respectively. Let P_{i0}, P_{j0}, P_{k0}, P_{l0} represent the original power flows, i.e., the power flows before A fails, on branches i, j, k, l, respectively. I_A can be considered as a function of the original power flow, which is expressed as:

$$I_A=f\left(P_{i0},P_{j0},P_{k0},P_{l0},P_{mk},P_{ml}\right) \tag{8}$$

In (8), P_{mk} and P_{ml} can be considered as constants; and P_{i0}, P_{j0}, P_{k0}, and P_{l0} depend on the state of the system before A fails. Since B and A are independent, the outages of B cannot affect the inputs of $f(\cdot)$. That is, the outage of B cannot affect I_A. Similarly, the outage of A cannot affect I_B. In this case, the sum of I_A and I_B is equal to $I_{A\cup B}$.

Based on the impact-increment-based reliability index calculation model and impact superposition theorem, we can propose an impact increment theorem (the corresponding proof process is presented in Appendix A): if A and B are independent, the impact increment of $A\bigcup B$ is 0.

According to the impact increment theorem, if the outage branches of a branch outage state can be decoupled into two independent branch sets, the impact increment of this state is 0. According to (2), when the impact increment is 0, the modified impact-increment is 0. That is, the modified impact-increment of this contingency state can be obtained directly without using OPF analysis.

The example system in Fig. 2 can be used to showcase the benefit of the impact increment theorem. Let R_3 represent the reliability index of the system. It can be expressed as:

$$\begin{aligned}R_3=&P_{\{1\}}I_{\{1\}}+P_{\{2\}}I_{\{2\}}+P_{\{3\}}I_{\{3\}}+P_{\{1,2\}}I_{\{1,2\}}+P_{\{1,3\}}I_{\{1,3\}}+P_{\{2,3\}}I_{\{2,3\}}+\\&P_{\{1,2,3\}}I_{\{1,2,3\}}=P_{\{1\}}\Delta I'_{\{1\}}+P_{\{2\}}\Delta I'_{\{2\}}+P_{\{3\}}\Delta I'_{\{3\}}+P_{\{1,2\}}\Delta I'_{\{1,2\}}+\\&P_{\{1,3\}}\Delta I'_{\{1,3\}}+P_{\{2,3\}}\Delta I'_{\{2,3\}}+P_{\{1,2,3\}}\Delta I'_{\{1,2,3\}}\end{aligned} \tag{9}$$

where $P_{\{\cdot\}}$ is the outage probability of branch set $\{\cdot\}$; and $\Delta I'_{\{\cdot\}}$ is the modified impact increment of branch set $\{\cdot\}$. The right side of the first equal sign is the traditional calculation model. The right side of the second equal sign is the impact-increment-based reliability index calculation model. Since $\{1\}$ is independent of $\{2\}$, $\{3\}$, and $\{2,3\}$, respectively, we can directly obtain the modified impact increments $\Delta I'_{\{1,2\}}$, $\Delta I'_{\{1,3\}}$, and $\Delta I'_{\{1,2,3\}}$. In this way, the impact-increment-based reliability index calculation model can be simplified as:

$$R_3=P_{\{1\}}\Delta I'_{\{1\}}+P_{\{2\}}\Delta I'_{\{2\}}+P_{\{3\}}\Delta I'_{\{3\}}+P_{\{2,3\}}\Delta I'_{\{2,3\}} \tag{10}$$

Equation (10) has fewer terms compared with the models in (9). Therefore, the number of OPF analyses in transmission reliability assessment can be reduced.

To determine whether outage branches can be decoupled, we need to obtain branch relations. Branch relations can be estimated by calculating power flow variation ratios. According to the definition, if there is a branch k (k can be the same branch as i or j), and the power flow variation ratios on branch k satisfy (11), then branches i and j are dependent.

$$\min\left\{\left|\frac{P_{k0}-P_{ki}}{P_{k0}}\right|,\left|\frac{P_{k0}-P_{kj}}{P_{k0}}\right|\right\}>0 \tag{11}$$

where P_{ki} and P_{kj} are the power flows on branch k when branches i and j fail, respectively. If no branch can satisfy (11), branches i and j are independent. Inequality (11) can be used as the estimation criteria of branch relations. The number on the right side of (11) is the branch-independence threshold. Due to the network structure of the transmission system, when a branch fails, the power flow variation ratios

on the other branches are usually greater than 0, which means that there is power flow coupling between most branches. In large-scale transmission systems, most of the coupling strengths, i.e., the power flow variation ratios, are less than 5%. Since two branches with a coupling strength less than 5% can approximately satisfy the impact superposition property, we can consider that the coupling is weak enough, and the corresponding modified impact increment is 0. Accordingly, we can replace 0 in (11) with the more appropriate threshold, i.e., 5%, to obtain higher efficiency without affecting accuracy.

Based on the above analysis, the relations between all branches in the system can be obtained and recorded in a matrix, namely the system independence matrix. The system independence matrix is a symmetric matrix containing only 0 and 1. The order of the matrix is equal to the number of branches in the system. Let m_{ij} represent the element of the i^{th} row and j^{th} column of the matrix. If branch i and branch j are independent, m_{ij} and m_{ji} are equal to 0; otherwise, m_{ij} and m_{ji} are equal to 1. The matrix establishment, i.e., branch relation estimation, contains the following steps.

Step 1: input the original power flow data and the branch-independence threshold λ. Initialize two n_b-order square matrices $\boldsymbol{M}_1$ and $\boldsymbol{M}_2$ with all elements of 0, where n_b is the number of branches in the system. Initialize two counters $i_c=0$ and $j_c=0$.

Step 2: set $i_c=i_c+1$. Let branch i_c out of service and calculate the updated power flow of all branches by performing a DC power flow analysis. Compute the power flow variation ratios of all branches and replace the i_c^{th} row of $\boldsymbol{M}_1$ with the vector of the power flow variation ratios.

Step 3: if $i_c<n_b$, go back to *Step 2*; otherwise, go to *Step 4*.

Step 4: set the elements in $\boldsymbol{M}_1$ larger than λ to be 1, and the rest to be 0.

Step 5: set $j_c=j_c+1$. Set $k_c=j_c$.

Step 6: set $k_c=k_c+1$. Add the k_c^{th} row vector of $\boldsymbol{M}_1$ to the j_c^{th} row vector. If the sum vector contains the elements greater than 1, $m_{j_ck_c}$ and $m_{k_cj_c}$ in $\boldsymbol{M}_2$ are set to be 1.

Step 7: if $k_c<n_b$, go back to *Step 6*; otherwise, go to *Step 8*.

Step 8: if $j_c<n_b$, go back to *Step 5*; otherwise, stop the process. The obtained matrix $\boldsymbol{M}_2$ is the system independent matrix.

After obtaining the system independence matrix, we can determine whether the outage branches of a contingency state can be decoupled. The determination of branch decoupling based on a contingency state example is illustrated in Fig. 3.

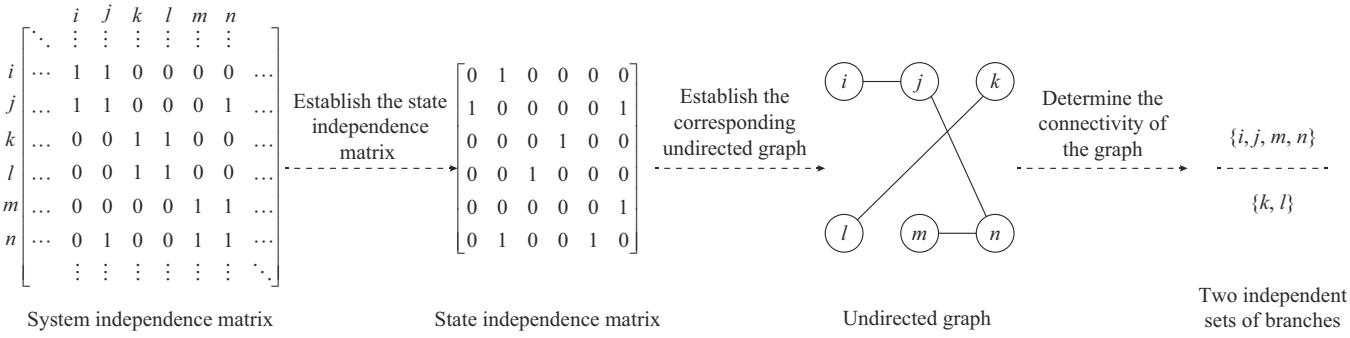

Fig. 3. Illustration of determination of branch decoupling based on a contingency state example.

Let $\{i,j,k,l,m,n\}$ represent the contingency state example, where i, j, k, l, m, and n are the outage branches of this state. The elements in the specific positions of the system independence matrix correspond to the relations between the outage branches. For instance, the element of the i^{th} row and j^{th} column of the system independence matrix is 1, indicating that branches i and j are dependent. The relations between the outage branches are recorded in a new matrix, namely the state independence matrix. The diagonal elements of this matrix are set to be 0. The contingency state corresponds to an undirected graph. The outage branches are regarded as the vertices of the graph. If two branches are independent, there is no edge between the corresponding two vertices. Conversely, if two branches are dependent, there is an edge between the corresponding two vertices. From the graph, we can find that there is no power flow coupling between $\{i,j,m,n\}$ and $\{k,l\}$. That is, $\{i,j,m,n\}$ and $\{k,l\}$ are independent. Therefore, the fact that the outage branches of this state can be decoupled is equivalent to the fact that the undirected graph is disconnected. The connectivity of an undirected graph can be determined by analyzing the corresponding state independence matrix. The process is as follows. First, the state independence matrix is established based on the system independence matrix. The state independence matrix is a symmetric matrix containing only 0 and 1. The order of the matrix is equal to the outage order of the contingency state. Let d_{ij} represent the element of the i^{th} row and j^{th} column of the matrix. If branch i and branch j are independent, d_{ij} and d_{ji} are equal to 0; otherwise, d_{ij} and d_{ji} are equal to 1. The diagonal elements of this matrix are set to be 0. The state independence matrix is actually the adjacency matrix of the undirected graph. Thereafter, the state independence matrix, i.e., the adjacency matrix, is transformed into the reachable matrix using Floyd algorithm. If all the elements in the reachable matrix are 1, the undirected graph is connected; otherwise, the undirected graph is disconnected.

According to the estimation of branch relations and the determination of branch decoupling, the BD technique requires n_b times DC power flow analyses and m_s times Floyd analyses during the simulation, where m_s is the number of sam-

pled contingency states. In contrast, the benefit of BD technique far outweighs its cost, which can be explained from two aspects. First, the BD technique avoids a large number of OPF analyses by taking advantage of the weak coupling between some branches. And the number of DC power flow analyses required by BD technique is only equal to the number of branches. Therefore, the number of reduced OPF analyses is much greater than that of increased DC power flow analyses. Second, the Floyd analysis is not time-consuming.

It should be noted that the BD technique cannot handle the first-order states. Therefore, if the sample space contains the first-order states, it is inevitable to repeatedly perform OPF analysis on the first-order states during the simulation, which puts a burden on the computation.

B. SSP Technique

To further improve the computational efficiency, the SSP technique is developed to separate lower-order states from the sample space. The normal state and first-order states are considered as the the lower-order states. The remaining states are the higher-order states. In general, the number of lower-order states is much smaller compared with higher-order states. The cumulative probability of lower-order states is higher than that of higher-order states. With the SSP technique, all lower-order states are enumerated, and the higher-order states are sampled.

The SSP technique can reduce the number of OPF analyses further, which can be explained from two aspects. First, since first-order states are no longer sampled, a higher proportion of sampled contingency states can satisfy the impact-increment theorem. The modified impact increments of these states can be obtained directly. Second, separating lower-order states from the sample space can greatly reduce the sample size needed for convergence, thus cutting down the number of sampled contingency states. The sample size reduction is confirmed by the sample size reduction theorem, which is proposed as follows. Let N_0 represent the sample size required by IIMCS to meet a given stopping criterion. Let N represent the sample size required to meet the same stopping criterion under the condition that lower-order states are separated from the sample space. We can obtain:

$$\frac{N_0}{N} \geq \frac{1}{1-P_L} \tag{12}$$

where P_L is the cumulative probability of all lower-order states.

According to (12), the lower bound of the sample size reduction is increased with the increase of P_L. The value of P_L depends on the component unavailability and system scale. In general, the order of magnitude of the branch unavailability is −3. If a transmission system has 200 components and the component unavailability is 0.005, P_L will be 0.7358. For 300 components with the same unavailability, P_L will be 0.5574. Therefore, the lower-order states have a relatively high cumulative probability. The effect of the sample size reduction is significant.

To make the reliability index accuracy not affected by the separation of the lower-order states, the SSP technique takes into account the contributions of the lower-order states on reliability indices by adding enumeration calculation. Due to the tiny number of the lower-order states, the amount of enumeration computation added by the SSP technique is much smaller than the amount of simulation computation reduced by the SSP technique. Therefore, the SSP technique can significantly improve computational efficiency.

Another advantage of SSP technique is its complementarity with BD technique. With the system scale decreases, the cumulative probability of the lower-order states increases, and the branch coupling becomes stronger, which weakens the OPF reduction capacity of BD. In comparison, the increase of the cumulative probability of lower-order states enhances the OPF reduction capacity of SSP technique. The complementary nature of BD and SSP makes BIRA well suited for systems with different scales.

C. Reliability Index Formulation

To accommodate the SSP technique, a new reliability index formulation is deduced based on (1). Since the SSP technique combines the lower-order state enumeration and higher-order state simulation, this new formulation can be expressed as a superposition of the formulations of these two parts. The formulation of each part is a conditional expectation multiplied by the corresponding probability weight. The new formulation of reliability index R can be expressed as:

$$\begin{aligned} R = E\left(\Delta I_s' | s \in S\right) = P_L E\left(\Delta I_s' | s \in S_L\right) + \\ \left(1-P_L\right) E\left(\Delta I_s' | s \in S_H\right) = P_L R_L + \left(1-P_L\right) R_H \end{aligned} \tag{13}$$

where S_H is the higher-order subspace; S_L is the lower-order subspace; $1-P_L$ is the cumulative probability of the higher-order states, i.e., the probability weight of the higher-order subspace; and R_L and R_H are the conditional expectations based on S_L and S_H, respectively. P_L, R_L, and R_H are given by:

$$P_L = \sum_{s \in S_L} P_s \tag{14}$$

$$R_L = E\left(\Delta I_s' | s \in S_L\right) = \frac{1}{P_L} \sum_{s \in S_L} P_s \Delta I_s' \tag{15}$$

$$R_H = E\left(\Delta I_s' | s \in S_H\right) = \frac{1}{1-P_L} \sum_{s \in S_H} P_s \Delta I_s' \approx \frac{1}{N} \sum_{i=1}^{N} \Delta I_{s(i)}' \quad s(i) \in S_H \tag{16}$$

where $s(i)$ is the i^{th} sample of state s, which is sampled based on the conditional probability $P_s/(1-P_L)$.

By substituting (15) and (16) into (13), we can obtain:

$$\begin{aligned} R = P_L R_L + \left(1-P_L\right) R_H \approx \sum_{s \in S_L} P_s \Delta I_s' + \\ \left(1-P_L\right) \frac{1}{N} \sum_{i=1}^{N} \Delta I_{s(i)}' \quad s(i) \in S_H \end{aligned} \tag{17}$$

The approximate equal sign in (17) indicates that the results obtained by BIRA are the estimated values of the true reliability indices. The estimated values are accurate and credible when a strict stopping criterion is satisfied.

D. Process of Reliability Index Computation Using BIRA

The BIRA consists of the state selection technique, i.e., the SSP technique, the state screening technique, i.e., the BD

technique, the state analysis algorithm, i. e., the OPF algorithm, and the new reliability index formulation. The process of reliability index computation using BIRA is illustrated in Fig. 4, where β_{EENS} and $\beta_{EENS,con}$ are the variation coefficient of the expected energy not supplied (EENS) estimator and the given stopping threshold, respectively.

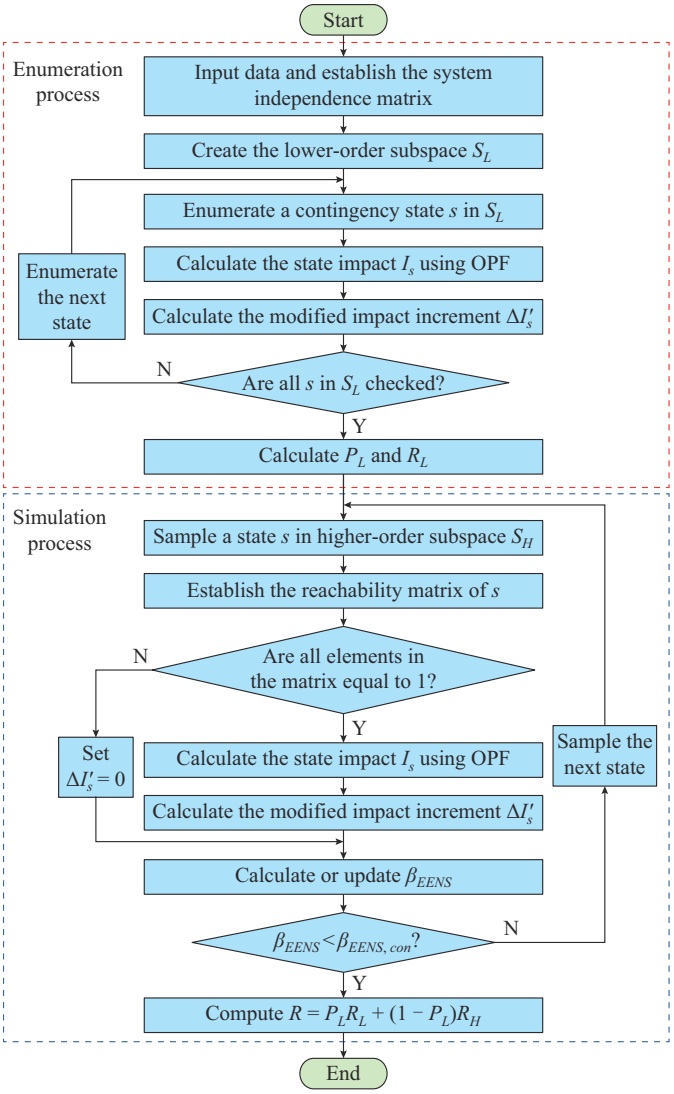

Fig. 4. Process of reliability index computation using BIRA.

IV. Case Study

The validity and applicability of BIRA are verified based on IEEE 118-bus and IEEE 145-bus test systems in Matpower 7.1. In contrast to the reliability assessment of the composite generation and transmission system, the reliability assessment of the transmission system focuses on the influence of branch outages on power adequacy [1]. Therefore, we suppose that the generation units of the test systems are 100% reliable. All branches have the same availability, i.e., the average of the branch availability of the IEEE reliability test system [22].

Our case studies focus on the two most concerned reliability indices, namely EENS and probability of load curtailments (PLC). During the simulation process, when β_{EENS} is less than a given stopping threshold, the simulation should be stopped. The stopping thresholds of the simulation methods (including MCS, IIMCS, and BIRA) are all set to be 0.05, and the independence threshold of BIRA is set to be 5%. The results obtained under a very strict stopping threshold, i.e., $\beta_{EENS,con} = 0.01$, are considered as the benchmarks. If the relative error between the result of a method and the corresponding benchmark is less than 5%, we consider the result to be precise. In the following case studies, we first determine whether the methods can satisfy the accuracy requirement. After that, the methods that cannot meet the accuracy requirement are excluded and the computational efficiency of the remaining methods is compared.

A. Case Study on IEEE 118-bus Test System

Table I illustrates the accuracy of annualized reliability indices obtained by different methods in IEEE 118-bus test system, where (1) and (2) represent the enumeration order. The annualized reliability indices are calculated based on the peak load level. With the same enumeration order, the reliability index accuracy of IISE is much higher than that of SE. This is because IISE transfers partial impacts of the higher-order states to the corresponding lower-order ones, which increases the contributions of the enumerated states to reliability indices. The EENS error of IISE(2) is 9.56%. With the increase of enumeration order, this error will be less than 5%. However, more than one million OPF analyses are required by IISE(3). Therefore, it is impractical for the enumeration methods to obtain accurate solutions. In contrast, the simulation methods (including MCS, IIMCS, and BIRA) can satisfy the accuracy requirement with an acceptable amount of computation. The differences between their reliability index errors are due to the randomness of statistics.

TABLE I
Accuracy of Annualized Reliability Indices Obtained by Different Methods in IEEE 118-bus Test System

Method	EENS (MWh/year)	EENS error (%)	PLC (%)	PLC error (%)	$\beta_{EENS,con}$
Benchmark	967.66		0.69		0.01
SE(1)	245.87	74.59	0.18	73.91	
SE(2)	580.59	40.00	0.38	44.93	
IISE(1)	820.23	15.24	0.64	7.25	
IISE(2)	875.13	9.56	0.68	1.45	
MCS	936.11	3.26	0.69	0	0.05
IIMCS	990.49	2.36	0.69	0	0.05
BIRA	989.05	2.21	0.69	0	0.05

Table II illustrates the accuracy of annual reliability indices obtained by different methods in IEEE 118-bus test system. The annual indices are calculated based on an 8-level load model. The load model is created from the 8736-hour load duration curve [24]. The 30% peak load is used as the lowest level. The load increment for the later levels is 10% peak load. By comparing Table I and Table II, we can find that the enumeration methods, i.e., SE and IISE, are more accurate in calculating annual indices than in calculating annu-

alized indices. This is because the system with the 8-level load model is more reliable than that with peak load. In contrast, the accuracy of the sampling methods is not affected by the system reliability.

TABLE II
ACCURACY OF ANNUAL RELIABILITY INDICES OBTAINED BY DIFFERENT METHODS IN IEEE 118-BUS TEST SYSTEM

Method	EENS (MWh/year)	EENS error (%)	PLC (%)	PLC error (%)	$\beta_{EENS,con}$
Benchmark	460.89		0.38		0.01
SE(1)	199.35	56.75	0.19	50.00	
SE(2)	357.14	22.51	0.32	18.75	
IISE(1)	360.20	21.85	0.33	13.16	
IISE(2)	430.64	6.56	0.38	0	
MCS	448.15	2.76	0.38	0	0.05
IIMCS	446.49	3.12	0.38	0	0.05
BIRA	450.65	2.23	0.38	0	0.05

Table III illustrates the computational efficiency of different methods based on annualized reliability index calculation in IEEE 118-bus test system. The computational efficiency is quantified by CPU time. Compared with MCS, the computational efficiency of IIMCS is improved by 27.53%. This is because IIMCS reduces the sample size by lowering simulation variance. The sample size reduction can cut down the number of OPF analyses. Compared with IIMCS, the computational efficiency of BIRA is 73.83 times higher. This is because BIRA avoids repetitive OPF analyses of the first-order states and omits the OPF analyses of a part of the higher-order states. The BIRA is composed of the BD and SSP techniques. To fully demonstrate the effect of BD and SSP techniques, we implement the two techniques separately. The BD in the table represents the method after the SSP technique is disabled. This method is essentially the combination of BD technique and IIMCS method. By comparing BD method with IIMCS method, we can find that the BD method has an approximately equal sample size but fewer OPF analyses. This is because, by implementing BD technique, the OPF analyses of a proportion of sampled contingency states can be omitted. Since branch decoupling determination is not time-consuming, the CPU time cost by BD technique is branch relation estimation time. The branch relation estimation time is only 3 s. The simulation time saved by BD technique is 521 s. Therefore, the time saved by BD technique is much larger than the time cost by BD technique. The SSP in the table represents the method after the BD technique is disabled. This method is essentially the combination of the SSP technique and IIMCS method. Compared with IIMCS, the SSP method has a much smaller sample size and number of OPF analyses. This is because replacing lower-order simulation with lower-order enumeration can significantly reduce the sample size and the number of OPF analyses. The simulation time saved by SSP technique is 2102 s. The enumeration time cost by SSP technique is only 7 s. Therefore, the time saved by SSP technique is much larger than the time cost by SSP technique. Compared with BD technique, the effect of SSP technique is more significant. This is because the cumulative probability of the lower-order states of the IEEE 118-bus test system is relatively high. According to the sample size reduction theorem, the sample size reduction and the cumulative probability are positively correlated.

TABLE III
COMPUTATIONAL EFFICIENCY OF DIFFERENT METHODS BASED ON ANNUALIZED RELIABILITY INDEX CALCULATION IN IEEE 118-BUS TEST SYSTEM

Method	Sample size	Number of sampled contingency states	Number of OPF analyses	CPU time (s)			
				Branch decoupling	Enumeration	Simulation	Total
MCS	163687	73100	73100			2863	2863
IIMCS	130825	58622	58622			2245	2245
BD	131986	58910	45197	3		1724	1727
SSP	3605	3605	3791		7	143	150
BIRA	3610	3610	651	3	7	20	30

Table IV illustrates the computational efficiency of different methods based on annual reliability index calculation in IEEE 118-bus test system. It can be observed that the efficiency of the simulation methods in calculating annual indices is lower than that in calculating annualized indices. This is because the sampling efficiency of MCS usually decreases with the improvement of system reliability. For MCS, IIMCS, and SSP, the number of OPF analyses is higher than that of sampled contingency states. This is because, for each sampled contingency state, it is necessary to obtain the state impact at each load level. If the state impact with peak load is not 0, the state should be further analyzed using OPF at the lower load level.

The BIRA method involves two preset parameters, i. e., the stopping threshold $\beta_{EENS,con}$ and branch-independence threshold λ. The value of $\beta_{EENS,con}$ determines whether the method converges when the simulation stops. The convergence contains two meanings, i. e., credibility and accuracy. Due to the randomness of statistics, the reliability assessment under a non-strict threshold still has the probability of obtaining accurate results. However, if the evaluation is repeated several times under this threshold, the results may be dramatically different, making the results lack credibility. To fully illustrate the effect of $\beta_{EENS,con}$ on the convergence of BIRA, we select different $\beta_{EENS,con}$ and perform ten times evaluations under each $\beta_{EENS,con}$. The convergence process can be described by the distributions of reliability index errors. Figure 5 illustrates the distributions of reliability index errors corresponding to different $\beta_{EENS,con}$ in IEEE 118-bus test system.

TABLE IV
COMPUTATIONAL EFFICIENCY OF DIFFERENT METHODS BASED ON ANNUAL RELIABILITY INDEX CALCULATION IN IEEE 118-BUS TEST SYSTEM

Method	Sample size	Number of sampled contingency states	Number of OPF analyses	CPU time (s)			
				Branch decoupling	Enumeration	Simulation	Total
MCS	263162	118120	123585			5566	5566
IIMCS	294907	131980	138503			6051	6051
BD	293378	131509	106802	3		4405	4408
SSP	5276	5276	6131		7	224	231
BIRA	5212	5212	1245	3	7	41	51

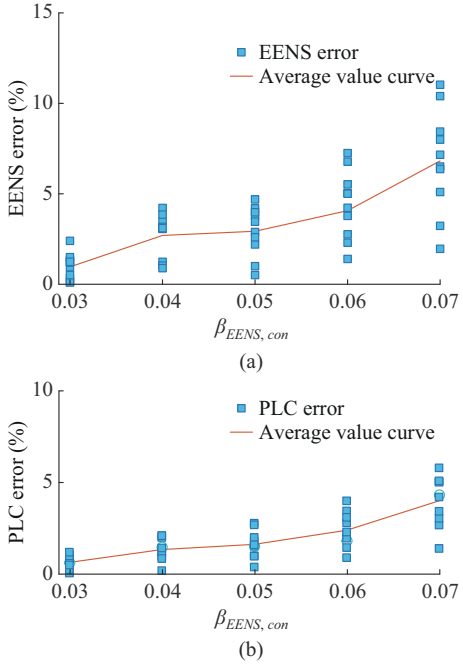

Fig. 5. Distribution of reliability index errors corresponding to different $\beta_{EENS,con}$ in IEEE 118-bus test system. (a) Distribution of EENS error corresponding to different $\beta_{EENS,con}$. (b) Distribution of PLC error corresponding to different $\beta_{EENS,con}$.

According to the distribution of EENS error in Fig. 5(a), the fluctuation of EENS error decreases with the decrease of $\beta_{EENS,con}$. Therefore, we can consider that the evaluation credibility increases with the decrease of $\beta_{EENS,con}$. Besides, with the decrease of $\beta_{EENS,con}$, the overall trend of EENS error is downward. The phenomenon can be verified by the downward trend of the average value. Therefore, with the decrease of $\beta_{EENS,con}$, the evaluation accuracy is improved. According to the above analysis, with the decrease of $\beta_{EENS,con}$, the convergence degree is improved. It should be emphasized that with the decrease of $\beta_{EENS,con}$, the computational burden increases. We should choose an appropriate stopping threshold to balance the convergence degree and computational efficiency. The comparison between Fig. 5(a) and Fig. 5(b) shows that the convergence speed of BIRA when calculating PLC is faster than that when calculating EENS. This is because, with the same sample size, the variation coefficient of the PLC estimator is less than that of the EENS estimator.

The branch-independence threshold λ determines the branch relation accuracy and further affects reliability index accuracy and computational efficiency. To eliminate the disturbance of statistical randomness, we only enumerate the second-order states and calculate the second-order EENS with different λ. The second-order EENS refers to the contribution of the second-order states to the entire EENS. When λ is equal to 0, no contingency states are screened out. Therefore, the EENS obtained with $\lambda = 0$ and the corresponding CPU time can be used as the benchmarks. Figure 6 illustrates the effects of λ on the second-order EENS error and computational efficiency in IEEE 118-bus test system. There is a positive correlation between λ and the computational efficiency. Similarly, λ and the EENS error are also positively correlated. When λ is set to be 5%, there is no error in EENS and the efficiency improvement is significant. In this case, we can get accurate reliability indices with high computational efficiency. As λ continues to increase, we can get higher computational efficiency at the cost of lower accuracy. However, when $\lambda > 10\%$, the EENS error increases exponentially as CPU time decreases. Therefore, to balance accuracy and efficiency, the threshold should not be larger than 10%.

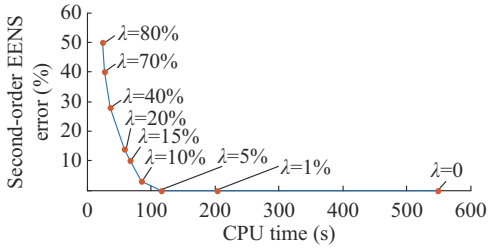

Fig. 6. Effects of λ on second-order EENS error and computational efficiency in IEEE 118-bus test system.

B. Case Study on IEEE 145-bus Test System

Table V illustrates the accuracy of annualized reliability indices obtained by different methods in IEEE 145-bus test system. The SE and IISE cannot meet the accuracy requirement. Besides, the reliability index errors of IEEE 145-bus test system are larger than those of IEEE 118-bus test system. This is because, with the increase of system scale, enumeration methods are more difficult to meet the accuracy requirement. In contrast, the simulation methods can meet the accuracy requirement with acceptable calculation time.

TABLE V
ACCURACY OF ANNUALIZED RELIABILITY INDICES OBTAINED BY DIFFERENT METHODS IN IEEE 145-BUS TEST SYSTEM

Method	EENS (MWh/year)	EENS error (%)	PLC (%)	PLC error (%)	$\beta_{EENS,con}$
Benchmark	7531.70		1.03		0.01
SE(1)	1500.78	80.07	0.20	79.61	
SE(2)	4064.70	46.03	0.56	45.63	
IISE(1)	6322.86	16.05	0.95	8.05	
IISE(2)	6700.95	11.03	1.01	1.94	
MCS	7698.15	2.21	1.02	0.90	0.05
IIMCS	7376.53	2.06	1.03	0	0.05
BIRA	7422.18	1.45	1.03	0	0.05

Table VI illustrates the computational efficiency of different methods based on annualized reliability index calculation in IEEE 145-bus test system. As an improved MCS method, the computational efficiency of IIMCS is 8.33% lower than that of MCS. This is because the effect of IIMCS depends on the state impact distribution of the evaluated system. IIMCS cannot reduce the simulation variance of the IEEE 145-bus test system. BIRA still performs well in computational efficiency. The computational efficiency of BIRA is 32.53 times higher than that of IIMCS. By comparing Table II and Table IV, we can find that the effect of BD technique becomes stronger. While for the SSP technique, the effect becomes weaker. This is because, with the increase of system scale, the branch coupling becomes weaker, which enhances the OPF reduction capacity of BD technique. Besides, with the increase of system scale, the cumulative probability of lower-order states decreases, which lowers the OPF reduction capacity of SSP technique. The complementary nature of BD and SSP techniques makes BIRA well suited for the systems with different scales.

TABLE VI
COMPUTATIONAL EFFICIENCY OF DIFFERENT METHODS BASED ON ANNUALIZED RELIABILITY INDEX CALCULATION IN IEEE 145-BUS TEST SYSTEM

Method	Sample size	Number of sampled contingency states	Number of OPF analyses	CPU time (s)			
				Branch decoupling	Enumeration	Simulation	Total
MCS	59140	46730	46730			1021	1021
IIMCS	64091	50622	50622			1106	1106
BD	63585	50225	18580	4		493	497
SSP	8058	8058	8511		11	185	196
BIRA	7998	7998	1143	4	11	19	34

V. CONCLUSION

This paper proposes a BIRA approach for transmission systems that consists of the BD and SSP techniques. The BD technique takes advantage of branch relations to screen out a proportion of sampled contingency states. The OPF analyses of these states can be omitted. Since BD technique cannot handle the first-order states, and the effect of BD technique decreases with the decrease of system scale, the SSP technique has been developed to compensate for the shortcomings of BD technique. The SSP technique can avoid repeated OPF analyses of the first-order states. In addition, with the decrease of system scale, the effect of SSP technique is enhanced. The good applicability of BIRA is achieved by the complementarity of BD and SSP techniques. The case studies on two different test systems have verified the validity and applicability of our approach.

APPENDIX A

According to mathematical induction, (3) can be further expressed as:

$$\Delta I_s = \sum_{k=1}^{n_s} (-1)^{n_s-k} \sum_{u \in \Omega_s^k} I_u = I_s - \sum_{k=1}^{n_s-1} \sum_{u \in \Omega_s^k} \Delta I_u \tag{A1}$$

In this paper, we use a set of outage branches to represent the corresponding branch outage state. If two branch sets are independent, the corresponding states are independent. Let n_o represent the outage order of $A \cup B$. When $n_o = 2$, according to (3) and the impact superposition theorem, we can obtain:

$$I_{A\cup B} - I_A - I_B = \Delta I_{A\cup B} = 0 \tag{A2}$$

where $\Delta I_{A\cup B}$ is the impact increment of $A \cup B$.

Suppose that in the case of $2 < n_o \le k$, $\Delta I_{A\cup B}$ is still equal to 0. Let i represent a branch and $A \cup \{i\}$ is independent of B. We can deduce that $\Delta I_{A\cup\{i\}\cup B}$ is equal to 0. The derivation process is as follows:

$$\begin{aligned}
\Delta I_{A\cup\{i\}\cup B} &= I_{A\cup\{i\}\cup B} - \sum_{k=1}^{n} \sum_{u \in \Omega_{A\cup\{i\}\cup B}^k} \Delta I_u = I_{A\cup\{i\}\cup B} - \\
&\left(\sum_{k=1}^{n_1} \sum_{u \in \Omega_{A\cup\{i\}}^k} \Delta I_u + \sum_{k=1}^{n_2} \sum_{u \in \Omega_B^k} \Delta I_u \right) = I_{A\cup\{i\}} + I_B - \\
&\left(\Delta I_{A\cup\{i\}} + \sum_{k=1}^{n_1-1} \sum_{u \in \Omega_{A\cup\{i\}}^k} \Delta I_u \right) - \left(\Delta I_B + \sum_{k=1}^{n_2-1} \sum_{u \in \Omega_B^k} \Delta I_u \right) = \\
&\left(I_{A\cup\{i\}} - \sum_{k=1}^{n_1-1} \sum_{u \in \Omega_{A\cup\{i\}}^k} \Delta I_u \right) - \left(\Delta I_{A\cup\{i\}} + \Delta I_B \right) + \\
&\left(I_B - \sum_{k=1}^{n_2-1} \sum_{u \in \Omega_B^k} \Delta I_u \right) = \Delta I_{A\cup\{i\}} - \left(\Delta I_{A\cup\{i\}} + \Delta I_B \right) + \Delta I_B = 0
\end{aligned} \tag{A3}$$

where n_1 is the outage order of $A \bigcup \{i\}$; and n_2 is the outage order of B.

According to (A3), when $n_o = k+1$, $\Delta I_{A \cup B}$ is equal to 0. The impact increment theorem is proven.

REFERENCES

[1] R. N. Allan, *Reliability Evaluation of Power Systems*. Berlin, Germany: Springer Science & Business Media, 2013.

[2] W. Li, *Risk Assessment of Power Systems: Models, Methods, and Applications*. New Jersey: John Wiley & Sons, 2014.

[3] H. Liu, Y. Sun, L. Cheng *et al*., "Online short-term reliability evaluation using a fast sorting technique," *IET Generation, Transmission & Distribution*, vol. 2, no. 1, pp. 139-148, Jan. 2008.

[4] H. Liu, Y. Sun, P. Wang *et al*., "A novel state selection technique for power system reliability evaluation," *Electric Power Systems Research*, vol. 78, no. 6, pp. 1019-1027, Jun. 2008.

[5] C. M. Davis and T. J. Overbye, "Multiple element contingency screening," *IEEE Transactions on Power Systems*, vol. 26, no. 3, pp. 1294-1301, Aug. 2011.

[6] Y. Jia, P. Wang, X. Han *et al*., "A fast contingency screening technique for generation system reliability evaluation," *IEEE Transactions on Power Systems*, vol. 28, no. 4, pp. 4127-4133, Nov. 2013.

[7] Z. Li, J. Wang, H. Sun *et al*., "Transmission contingency screening considering impacts of distribution grids," *IEEE Transactions on Power Systems*, vol. 31, no. 2, pp. 1659-1660, Mar. 2016.

[8] C. Fu and A. Bose, "Contingency ranking based on severity indices in dynamic security analysis," *IEEE Transactions on Power Systems*, vol. 14, no. 3, pp. 980-985, Mar. 1999.

[9] R. Billinton and X. Fang, "Selected considerations in utilizing monte carlo simulation in quantitative reliability evaluation of composite power systems," *Electric Power Systems Research*, vol. 69, no. 2, pp. 205-211, Jun. 2005.

[10] C. Singh and J. Mitra, "Composite system reliability evaluation using state space pruning," *IEEE Transactions on Power Systems*, vol. 12, no. 1, pp. 471-479, Feb. 1997.

[11] J. Mitra and C. Singh, "Pruning and simulation for determination of frequency and duration indices of composite power systems," *IEEE Transactions on Power Systems*, vol. 14, no. 3, pp. 899-905, Aug. 1999.

[12] D. Lieber, A. Nemirovskii, and R. Y. Rubinstein, "A fast Monte Carlo method for evaluating reliability indexes," *IEEE Transactions on Reliability*, vol. 48, no. 3, pp. 256-261, Sept. 1999.

[13] B. Hua, Z. Bie, S. Au *et al*., "Extracting rare failure events in composite system reliability evaluation via subset simulation," *IEEE Transactions on Power Systems*, vol. 30, no. 2, pp. 753-762, Sept. 2014.

[14] A. da Silva, R. Fernandez, and C. Singh, "Generating capacity reliability evaluation based on Monte Carlo simulation and cross-entropy methods," *IEEE Transactions on Power Systems*, vol. 25, no. 1, pp. 129-137, Feb. 2010.

[15] R. Fernandez, A. da Silva, L. Resende *et al*., "Composite systems reliability evaluation based on Monte Carlo simulation and cross-entropy methods," *IEEE Transactions on Power Systems*, vol. 28, no. 4, pp. 4598-4606, Nov. 2013.

[16] A. da Silva, L. Resende, L. Manso *et al*., "Composite reliability assessment based on Monte Carlo simulation and artificial neural networks," *IEEE Transactions on Power Systems*, vol. 22, no. 3, pp. 1202-1209, Feb. 2007.

[17] N. M. Pindoriya, P. Jirutitijaroen, and C. Singh, "Composite reliability evaluation using Monte Carlo simulation and least squares support vector classifier," *IEEE Transactions on Power Systems*, vol. 26, no. 4, pp. 2483-2490, Nov. 2011.

[18] D. Urgun and C. Singh, "A hybrid Monte Carlo simulation and multi label classification method for composite system reliability evaluation," *IEEE Transactions on Power Systems*, vol. 34, no. 2, pp. 908-917, Mar. 2019.

[19] Y. Lei, K. Hou, Y. Wang *et al*., "A new reliability assessment approach for integrated energy systems: using hierarchical decoupling optimization framework and impact-increment based state enumeration method," *Applied Energy*, vol. 210, no. 15, pp. 1237-1250, Jan. 2018.

[20] Y. Lei, P. Zhang, K. Hou *et al*., "An incremental reliability assessment approach for transmission expansion planning," *IEEE Transactions on Power Systems*, vol. 33, no. 3, pp. 2483-2490, May 2018.

[21] S. Hou, P. Zhang, K. Hou *et al*., "Contingency set partition-based impact transfer approach for the reliability assessment of composite generation and transmission systems," *International Journal of Electrical Power & Energy Systems*, vol. 122, pp. 1-11, Nov. 2020.

[22] Probability Methods Subcommittee, "IEEE reliability test system," *IEEE Transactions on Power Apparatus and Systems*, vol. 98, no. 6, pp. 2047-2054, Dec. 1979.

Shuonan Hou received the B.E. degree in electrical engineering and automation from Northwestern Polytechnical University, Xi'an, China, in 2008, and the M.S. degree in power systems and automation from Northeast University, Shenyang, China, in 2014. He is currently pursuing the Ph.D. degree in electrical engineering at Tianjin University, Tianjin, China. His research interests include reliability and risk assessment of power system, integrated energy system, and smart grid.

Pei Zhang received the Ph.D. degree from the Imperial College of Science, Technology, and Medicine, University of London, London, UK, in 1999. He is currently a Professor at Beijing Jiaotong University, Beijing, China. He was the Director leading smart grid activities at Accenture, Beijing, China. Before joining Accenture, he worked as the Program Manager responsible for grid operation and planning at Electric Power Research Institute (EPRI), Palo Alto, USA. His current research interests include power system stability and control, reliability and security assessment, and application of probabilistic methods to power systems.

Wei Zhang received the B.E. degree from Shandong University, Jinan, China, in 2013. He received the Ph.D. degree from the School of Microelectronics, Tianjin University, Tianjin, China, and the Department of Electronics, Carleton University, Ottawa, Canada, in 2020. He is currently an Associate Researcher with the School of Electronic engineering, Beijing University of Posts and Telecommunications, Beijing, China. His research interests include reliability and risk assessments of power system, smart grid, neural-network-based methods for microwave device modeling, space mapping, and surrogate model optimization.

Qian Xiao received the Ph.D. degree in electrical engineering from Tianjin University, Tianjin, China, in 2020. From Oct. 2018 to Nov. 2019, he was a Visiting Scholar with the Department of Energy Technology, Aalborg University, Aalborg, Denmark. He is currently an Associate Professor with the School of Electrical and Information Engineering, Tianjin University. His current research interests include microgrid, DC distribution network, multilevel converter and power electronics for distributed energy and energy router.

Xiaonan Liu received the Ph.D. degree in electrical engineering from Tianjin University, Tianjin, China, in 2021. She is currently working at State Grid Tianjin Electric Power Research Institute, Tianjin, China. Her research interests include reliability and resilience assessment of power systems.